High latitude solar heating using photovoltaic panels, air-source heat pumps and borehole thermal energy storage

Janne Hirvonen[1], Kai Sirén[1]

[1] Aalto University School of Engineering, Espoo (Finland)

Abstract

A solar community of 100 passive houses was designed for high latitude Finnish conditions. Typical solar thermal energy generation was replaced by solar electric system which was used to operate heat pumps. Short-term water-based thermal storage tanks were charged with an air-to-water heat pump and then discharged to a seasonal thermal storage system in the form of borehole thermal energy storage (BTES).

With total PV capacities of 240 to 600 kW, 78 to 97% of space heating and domestic hot water was provided by renewable energy from the local heating grid. Utilizing a water-to-water heat pump between low and high temperature water tanks increased the efficiency of the air-source heat pump. Varying the flow rate of borehole storage provided very minimal benefit.

Keywords: Solar community, seasonal thermal storage, solar electricity, heat pump,

1. Introduction

Solar energy availability varies between day and night and with seasons. The seasonal variability is different from country to country, with locations far from the equator experiencing larger changes in insolation. Finland is located above 60 °N latitude, which means that in summer the day can be 18 hours long, while in winter it might last only 6 hours. Correspondingly, energy demand for heating is greatest during winter, when there is little, if any, solar energy available. For this reason, conventional solar heating system with a short-term water storage is of limited utility in Finnish conditions. However, seasonal thermal storage may offer a solution.

Seasonal thermal storage allows the storage of heat for several months. The most popular seasonal storage methods are tank storage, aquifer storage, pit storage and borehole storage (Hesaraki, et al., 2015). Borehole thermal energy storage (BTES) consists of a grid of boreholes that have been drilled into the ground and fitted with heat transfer pipes (Lanahan & Tabares-Velasco, 2017). Hot fluid is circulated in the boreholes to heat the ground. If the size of the storage is large enough, thermal losses to the environment remain manageable and make it possible to provide a large fraction of heating by solar energy. Typically, the seasonal storage is heated by solar thermal collectors, which produce heat directly, as was the case in the Drake Landing Solar Community (Sibbitt, et al., 2012). Similar designs for Finnish conditions have been tested in an optimization study (Hirvonen, et al., 2017).

In Finland, the current market for solar thermal collectors is small, but installations of solar photovoltaic (PV) panels are accelerating and a new record for the country's largest PV system installation is set several times per year. Heat pumps are also replacing conventional district heating in many locations. Thus, combining these two technologies was considered in this paper. Solar electricity was used not only to meet the electric load of house appliances, but also to run an air-to-water heat pump to charge the seasonal thermal storage through a large water storage tank. The goal was to make an initial test of concept and find out the effect of different controls and solar generation capacity on the reduction of imported external energy.

2. Methodology and system description

This study looked at the energy matching in a virtual solar community of 100 single-family houses, located in Helsinki, Finland. The study was based on dynamic simulations performed with TRNSYS 17, using the weather data from Helsinki Test Reference Year 2010. The space heating (SH) demand in the houses was based on the

doi:10.18086/swc.2017.29.06 Available at http://proceedings.ises.org

simulated performance of a 100 m^2 passive level house with 25 kWh/m^2 annual energy demand according to heated floor area. The domestic hot water (DHW) demand was based on profiles gained from an IEA study (Jordan, 2001), normalized to 35 kWh/m^2. Electricity consumption of appliances was based on measured demand from 50 real district heated houses in the Helsinki region, normalized to 40 kWh/m^2.

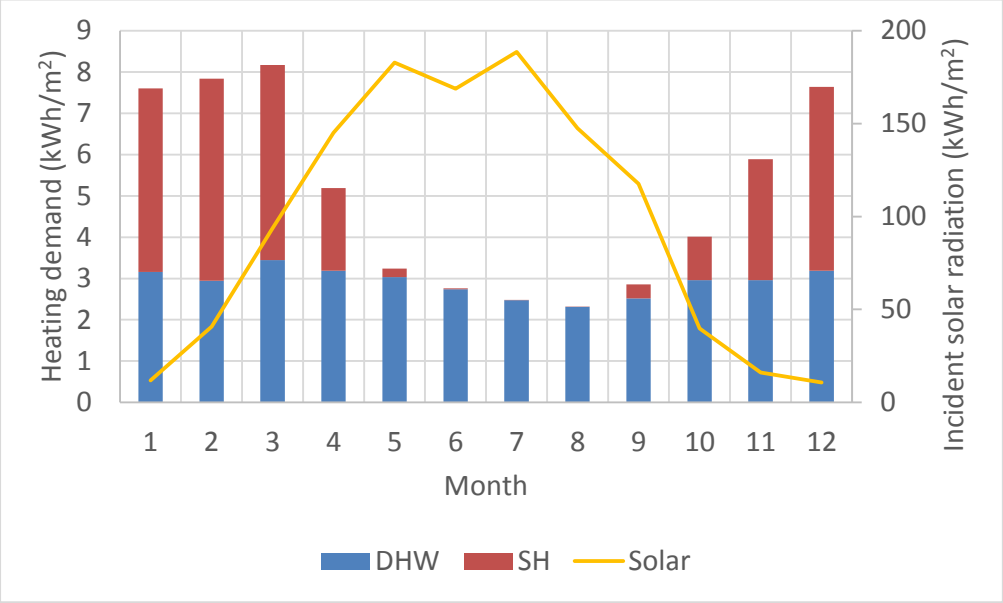

Figure 1: Monthly solar energy potential (vs. collector area) and heating demand in the houses of the community (vs. floor area).

The modeled energy system is shown in Figure 2. All the houses in the community were connected to a local heating grid that was fed from two large water storage tanks. The warm tank (300 m3) was used to supply space heating (SH) at 30 to 35 °C (floor heating) and to preheat the domestic hot water (DHW). The hot tank (150 m3) was used to superheat the DHW to the required temperature of 55 °C. The warm water tank was heated by an air-to-water heat pump (AW-HP, Figure 3) powered by solar photovoltaic (PV) panels, using ambient air as the heat source. The hot tank was heated by a water-to-water heat pump (WW-HP, Figure 4), using the warm tank as the heat source. Thus, the two heat pumps formed a type of cascade heat pump. Solar electricity was also used to run the house appliances. In case there was not enough solar power for all needs, the first priority of solar energy use was with the appliances, second priority with the WW-HP and third priority with the AW-HP. It was assumed that the heat pumps could be operated at any part-load between 10 and 100%. If solar electric power was not enough to run the AW-HP at the minimum part-load, the HP would not start. The ratios of the source-side (ambient air or warm water) and load-side flows (warm or hot water) in the heat pumps were kept constant. The flows adjusted according to heat pump power, to keep the load-side temperature change roughly constant at 12 °C.

If the warm tank cooled down and there was not enough solar energy available, it was be heated by discharging the seasonal storage. If the warm tank temperature rose above 50 °C by the use of the AW-HP, the extra heat was transferred to the seasonal storage. When the BTES temperature was above the tank temperature and the required SH temperature, energy from the ground was transferred back to the tank.

The seasonal storage was a borehole thermal energy storage system, contained in rock with thermal conductivity of 3.5 W/mK and total volume of 30 000 m3. There were 216 boreholes, each 37 m deep, evenly distributed along the BTES cross-section. The boreholes were connected in groups of 4, to generate a radial temperature distribution in the BTES. During charging, hot fluid entered from the center, flowed through 4 boreholes and exited at the edge of the BTES. During discharging, cold fluid entered from the edge and exited through the center. As it takes several years for a BTES system to reach stable conditions, a three-year simulation period was used. The results reported in this study were for the final year, on the assumption that long-term steady-state conditions had been achieved.

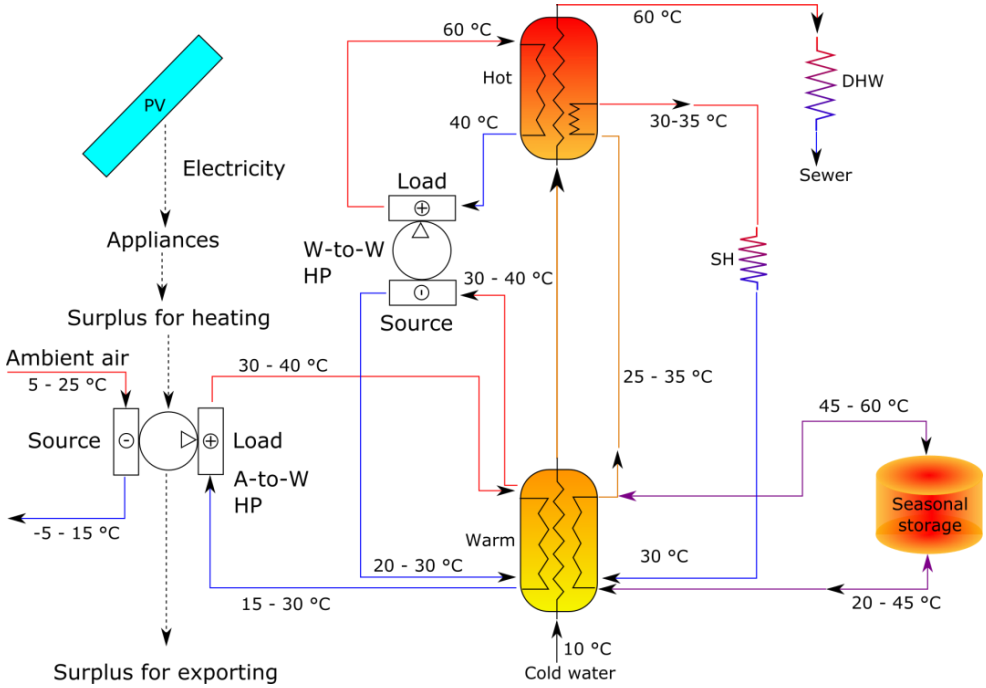

Figure 2: Energy system diagram.

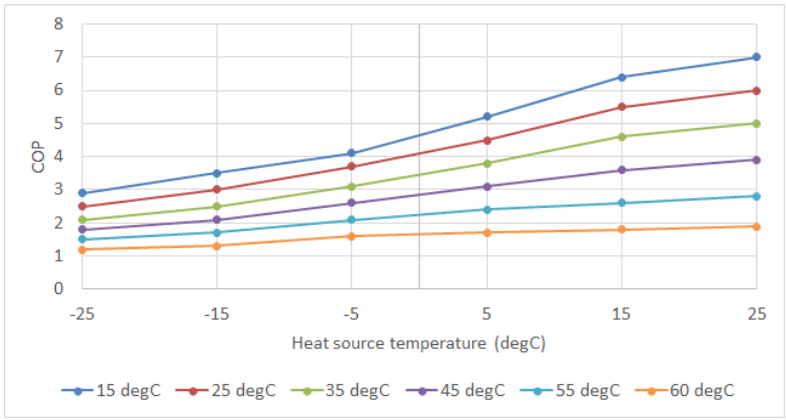

Figure 3: COP of the air-to-water heat pump with different load-side inlet temperatures. Based on model NIBE-2120.

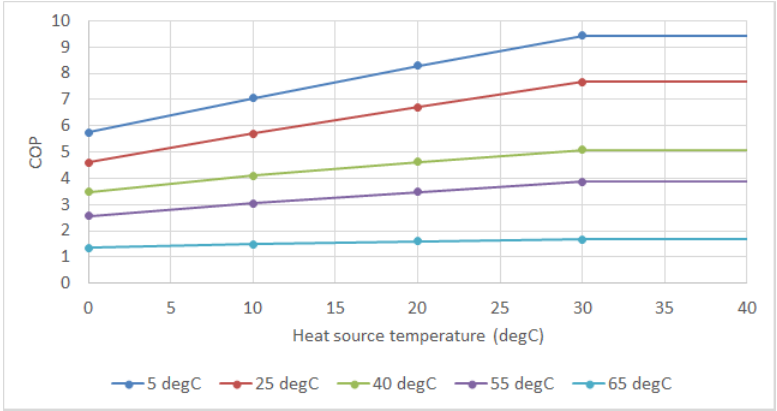

Figure 4: COP of the water-to-water heat pump with different load-side inlet temperatures. Based on model NIBE-F1345.

The total AW-HP thermal capacity was set to 960 kW, which corresponds to 240 kW electricity consumption in standard conditions. In addition, the WW-HP thermal capacity was set to 180 kW, which corresponds to 60 kW electricity consumption. Both heat pumps could be operated in part-load mode, with a minimum power of 10%. Actual ratio of thermal and electric ratio depended on the heat source temperature and load temperature, as shown in Figures 2 and 3.

2.1. Equations

Renewable energy fraction (REF) is the portion of end-use heat energy that is provided by the renewable energy of the local heating grid. Since electricity was the only external energy source, we can determine the REF indirectly

$$\mathrm{REF} = 1 - \frac{E_{imported\ heating\ elec}}{E_{SH}+E_{DHW}}, \qquad \text{(eq. 1)}$$

where $E_{\text{imported heating elec}}$ is the additional imported grid electricity needed for heating (heat pumps, backup system, pumps) after solar electricity has been accounted for, E_{SH} is the building-side space heating thermal energy demand and E_{DHW} is the building-side domestic hot water thermal energy demand. There was no electric energy storage, which limited the maximum amount of appliance related solar energy use. Thus, the REF only accounts for heating related energy, not electric appliances.

Efficiency of the seasonal storage is defined as the ratio of energy taken from the storage vs. the energy stored into the system

$$\eta_{\mathrm{BTES}} = \frac{E_{BTES\ discharge}}{E_{BTES\ charge}}. \qquad \text{(eq. 2)}$$

The PV system produces only electricity, but when connected to the heat pump the combined efficiency has the same meaning as the efficiency of a solar thermal collector. The combined thermal efficiency is defined as

$$\eta_{\mathrm{PV,thermal}} = COP_{HP}\frac{E_{PV,HP}}{G}, \qquad \text{(eq. 3)}$$

where COP_{HP} is the coefficient of performance for the heat pump, $E_{PV,HP}$ is the electricity consumed by the heat pump that was supplied by the PV system and G is the incident solar insolation on the solar panels.

2.2. Study parameters

To gain understanding of how the heating system and solar electricity interact, three parameters were chosen for analysis: PV capacity, BTES flow setting and WW-HP control mode.

PV capacity was selected as multiples of the nominal electricity consumption of the AW-HP (multiples 1, 1.5, 2, 2.5) to see how much excess capacity relative to the heating capacity is needed before there is enough power to both run the appliances and heat the BTES.

The BTES was operated in two different modes. In the Constant mode, all charging and discharging was done at a constant flowrate. In the Variable mode, the flowrate was changed according to the difference between the average BTES temperature and the temperature at the top of the warm tank. A high temperature difference corresponded to high flow and a low temperature difference to a low flow. The base flow rate for the BTES was 1600 kg/h per pipe loop. With a ΔT below 1, below 5, below 10 and above 10, the flow rate fraction was 25%, 50%, 75% and 100%, respectively.

The HP control setting decided whether the WW-HP was only run when the hot tank required recharging (setting 0) or if the hot tank was charged whenever there was available solar energy and the temperature at the top of the tank was less than 70 °C (setting 1). Additional use of the WW-HP lowers the temperature in the warm tank, thus increasing the COP of the air-to-water heat pump.

Table 1: Simulation parameters.

Case	PV capacity (kW)	BTES flow	HP control
0	0	-	0
1	240	Constant	0
2	240	Constant	1
3	240	Variable	0
4	240	Variable	1
5	360	Constant	0
6	360	Constant	1
7	360	Variable	0
8	360	Variable	1
9	480	Constant	0
10	480	Constant	1
11	480	Variable	0
12	480	Variable	1
13	600	Constant	0
14	600	Constant	1
15	600	Variable	0
16	600	Variable	1

3. Results

3.1. Renewable energy fraction

An important measure for energy system performance is the renewable energy fraction. Figure 5 shows the fraction of end-use heat energy that was met by the solar heating system. Even without any solar energy, 66% of heating was provided by the heat pump system alone. When solar capacity was set to 2.4 kW/house, which was equivalent to the maximum electricity use of the AW-HP, REF of heating was increased to 78%. Increasing the PV capacity to 3.6 kW/house, up to 88% REF was achieved. Increasing PV capacity further showed diminishing returns, as at 4.8 kW/house the maximum REF was 95% and at 6 kW/house it was 97%.

While PV capacity was the main determinant of REF, heat pump and BTES configurations also affected the results. With the smallest PV capacity (240 kW), increasing the WW-HP utilization during peak solar generation lowered REF compared to only running the WW-HP as needed by the hot tank. With all the larger solar generation capacities it had the opposite effect; increased use of WW-HP increased total REF. With a small PV capacity, the higher priority of the WW-HP prevented the operation of the AW-HP, since little extra solar energy was available for heating the warm tank and subsequently the BTES. With larger PV capacities there was enough energy to operate both the AW and WW heat pumps. In these cases, the WW heat pump cooled down the warm tank (which it used as an energy source), improving the COP of the AW-HP due to lower load-side temperatures. Increased use of WW-HP changed REF by -2.2%, +0.9%, +2,3% and +3.6% for the 240, 360, 480 and 600 kW cases, respectively. The effect of the variable BTES flow was less significant, though it was positive in all cases. The increase in heating REF was 0.2 to 0.6%, the largest gains found in the 360 kW case.

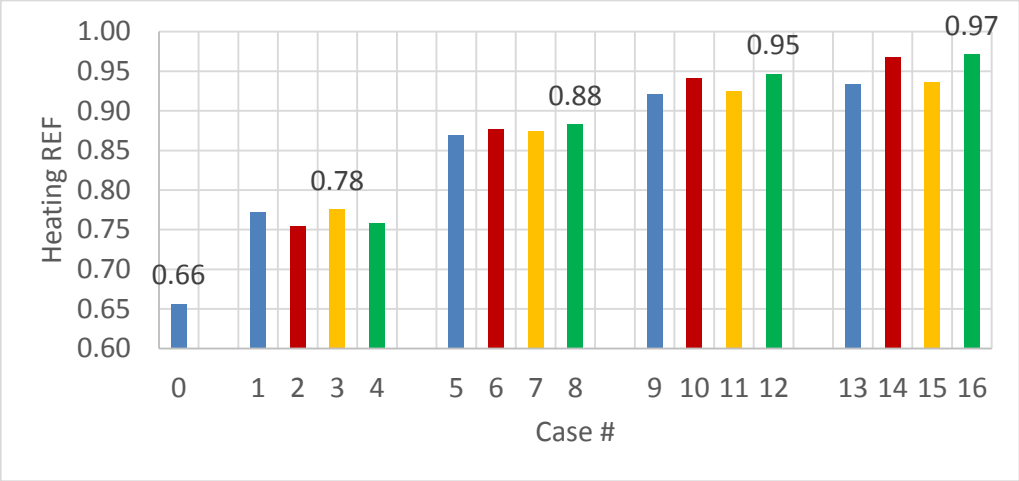

Figure 5: Annual renewable energy fraction of heating for the simulated cases. Bars with the same color have the same BTES and HP flow settings, but different PV capacity, as shown in Table 1. The numbers show the highest REF for each PV capacity.

3.2. Solar energy use

The solar energy generated by the PV panels was used for appliances, heat pumps and exporting. Increasing the PV capacity by 150% from 240 kW to 600 kW increased the PV use for appliances only by 25%, due to the mismatch in energy use and generation patterns. Most of the added solar energy generation was used by the AW-HP, as shown in Figure 6. Increasing the use of the WW-HP increased its electricity consumption by 230 to 420%, according to PV capacity. However, the total sum of the AW and WW heat pump electricity consumption remained practically constant in all the cases with the same PV capacity. In the cases with 240 and 360 kW PV capacity, 1% of PV generation was exported to the grid. With 480 and 600 kW, exports were 4 and 7% of PV generation.

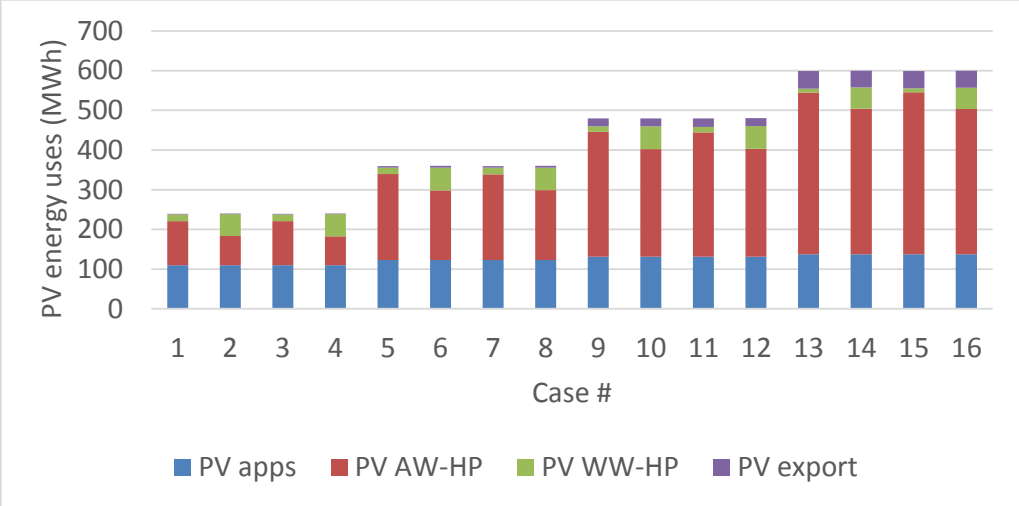

Figure 6: Annual distribution of PV generated energy for different uses.

3.3. Thermal efficiency of solar electric heat generation

Effective efficiency of solar panels when producing heat with heat pumps, hourly duration curve. Choose the best case of all PV sizes and put them in the same figure.

Since solar electricity was used to run the heat pumps, we can calculate the thermal efficiency of solar heat generation. Figure 7 shows the duration curves for the thermal efficiency of both heat pumps in the best cases of each PV capacity. The total running time of the AW heat pump was increased by adding more PV capacity, because after meeting appliance needs extra power was available more often. There was also a clear decrease in average efficiency as the PV capacity was increased. This is due to the AW HP operating at higher temperatures due to charging of the thermal storage tank. With WW HP, the longest running time and highest efficiency was

obtained in the 360 kW case. Conversely, the lowest efficiency was obtained with the 600 kW system.

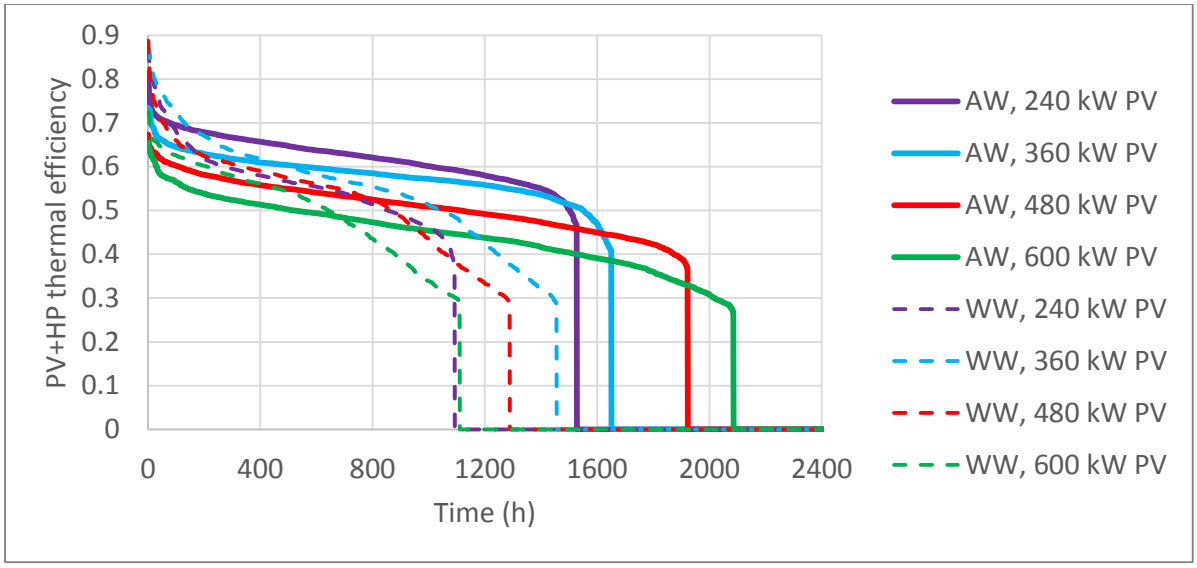

Figure 7: Duration curves of the thermal efficiency of heat pump energy generation using solar electricity.

3.4. BTES performance

Figure 8 shows the average temperature in the BTES during the seasonal cycle of the last simulated year. The bottom and top end of the bars represent the annual minimum and maximum temperatures, respectively. Also shown is the storage cycle efficiency. In the 240 kW PV cases, there was not enough energy to heat the BTES to the temperature levels required to meet space heating demand. The low temperature resulted in a very high cycle efficiency. Higher PV capacity raised the storage temperature.

The borehole flow setting had no practical effect on the temperature. The more active operation mode of the WW HP, however, decreased temperature and increased BTES efficiency for most cases. In the 360 kW cases, the lower temperature was also joined by lower efficiency.

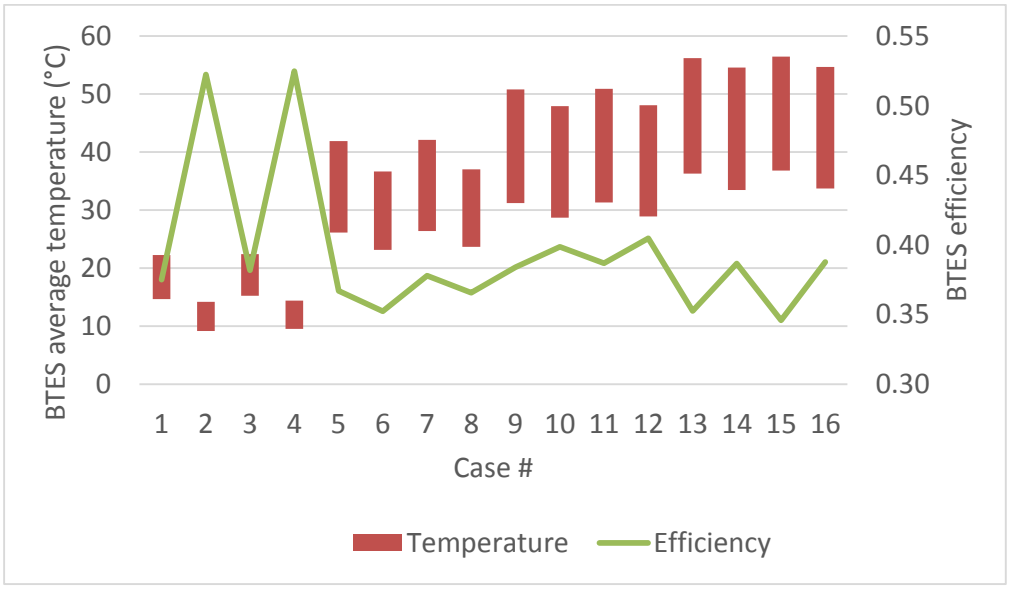

Figure 8: Range of average seasonal storage temperature and the annual seasonal storage efficiency.

3.5 Monthly comparison

Figure 9 shows the third year monthly electricity flows and seasonal storage temperatures in Case 1. Generation from the PV system was distributed between appliances, AW-HP and WW-HP. The minimum need for external energy happened in July, with 15 MWh of electricity imported. The maximum happened in December, with

66 MWh of electricity imported. The low amount of 2.4 kW solar panels per building didn't have enough excess energy to allow the charging of the seasonal storage. Thus, the maximum temperature achieved by the BTES was 22 °C, which was not enough to provide heating in winter.

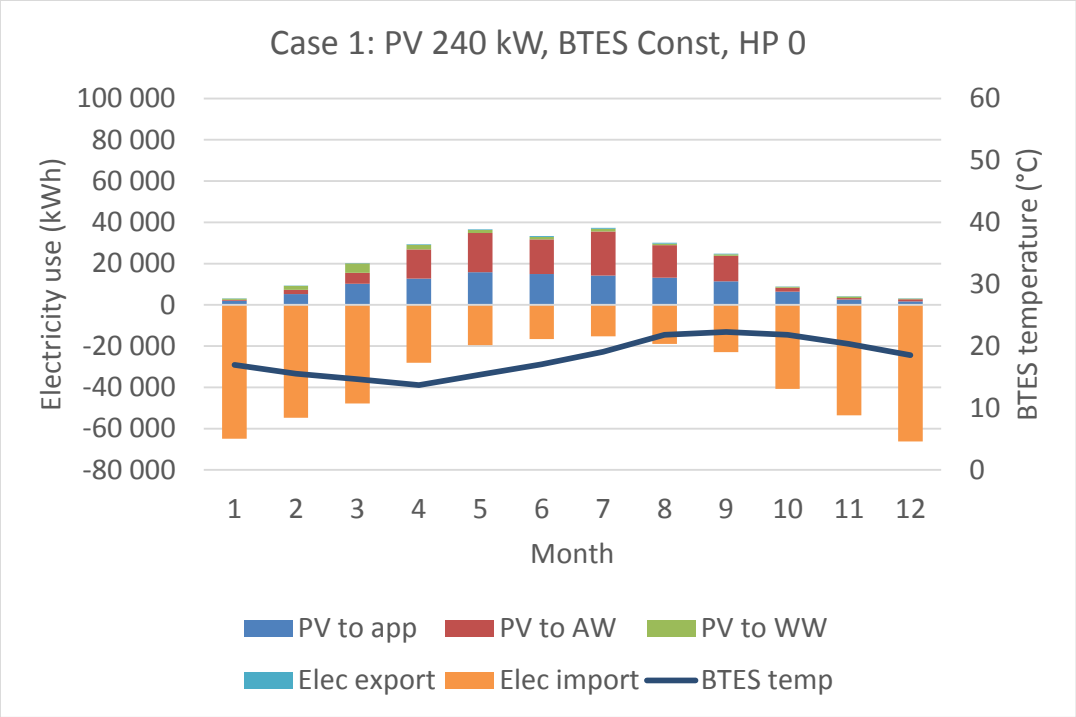

Figure 9: Electricity flows and seasonal storage temperatures in Case 1.

Figure 10 shows the third year monthly electricity flows and seasonal storage temperatures in Case 16. Now the higher solar capacity allowed diverting a large amount of solar electricity to the operation of the AW-HP. The extra heat was then used to charge the BTES up to 55 °C, while the annual cycle only dropped the temperature down to 34 °C. The need for imported energy was reduced compared to Case 1, as the minimum imports were 10 MWh in July and maximum 45 MWh in December. This highlights the difficulty of utilizing significant amounts of solar energy in high latitude conditions, which have a high seasonal mismatch in demand and generation. Increasing nominal solar energy capacity by 150%, compared to Case 1, reduced the need for external energy by only 32% during the peak month.

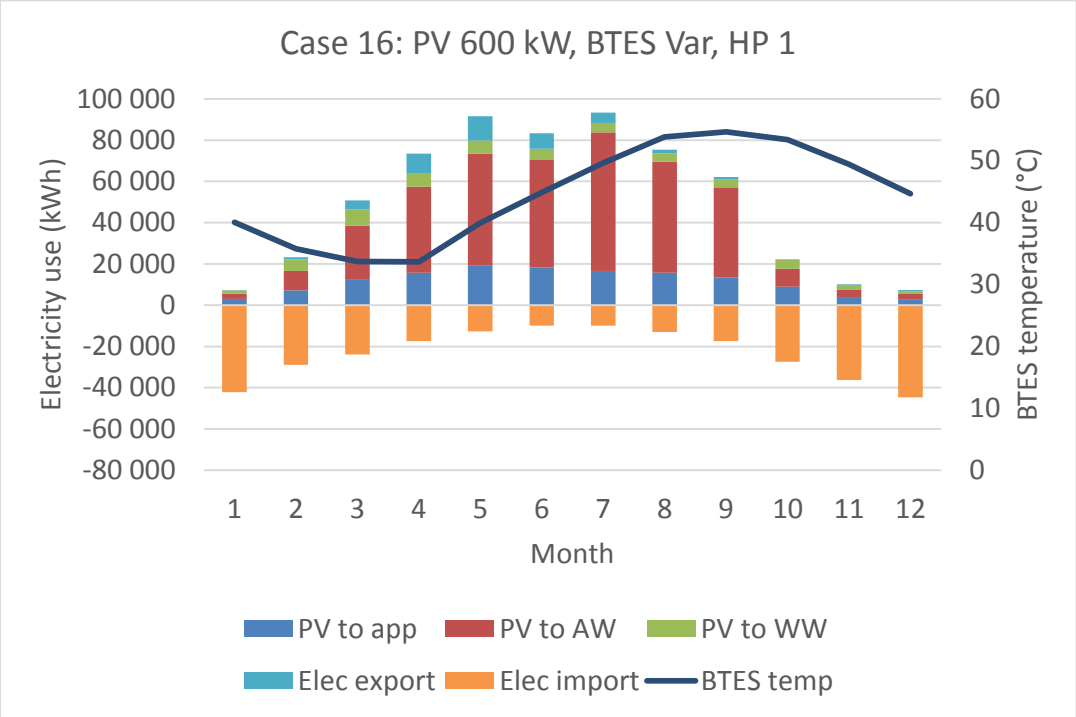

Figure 10: Electricity flows and seasonal storage temperatures in Case 16.

4. Discussion and conclusions

The heat pump based solar heating concept introduced in the paper worked well. A renewable energy fraction of up to 97% was achieved by having a nominal solar electric capacity of 600 kW. This was equal to 2.5 times the maximum electricity consumption of the air-to-water heat pump. However, even with a PV capacity of 360 kW, 1.5 times the maximum electric power of the AW-HP, the REF could be as high as 88%. Thus, with passive houses, a relatively low amount of PV generation per house was needed to achieve a high REF. Using the solar photovoltaic system simplifies the solar community design compared to a solar thermal collector design, because the same solar panels can supply both the heat and the electricity. In addition, no piping is required between the solar collectors and storage tanks.

Varying the BTES flowrate did not significantly influence the system performance. This implies that using a constant flow rate is effective enough, though the optimal flow rate could still be different than what was selected in this study.

Combined with the air-to-water heat pump, the average thermal efficiency of solar heat generation could be above 50%, even when heating REF was above 90%. The thermal efficiency of this electric heating system compared favorably to the 33% solar thermal efficiency obtained in the Drake Landing Solar Community (DLSC, 2012). Utilizing the water-to-water heat pump between the two buffer storage tanks increased total system efficiency by lowering the input temperature of the air-to-water heat pump, but only if PV capacity was large enough to also allow additional use of the AW heat pump. It should be noted that the ideal heat pump modeled here suffered no ill effects from part-load use or fast on-off behavior and could always adjust perfectly to the current solar conditions. A real-life system may face more difficulties in these aspects, which might lower total system efficiency.

A high REF solar community based on solar electricity and heat pumps was found to be technically feasible in a high latitude country like Finland. However, the seasonal energy mismatch and large losses in the seasonal thermal energy storage cause diminishing returns for increased solar capacities. Further optimization is needed to find out economical implementations of the basic design.

5. References

DLSC, 2012. *Drake Landing Solar Community, monthly reports.* [Online]
Available at: https://www.dlsc.ca/reports.htm
[Accessed 16 August 2017].

Hesaraki, A., Holmberg, S. & Haghighat, F., 2015. Seasonal thermal energy storage with heat pumps and low temperatures in building projects - A comparative review. *Renewable and Sustainable Energy Reviews,* pp. 1199-1213.

Hirvonen, J., Rehman, H. u., Deb, K. & Sirén, K., 2017. Neural network metamodelling in multi-objective optimization of a high latitude solar community. *Solar Energy,* Volume 155, pp. 323 - 335.

Jordan, U., 2001. *Realistic domestic hot-water profiles in different time scales,* Marburg: International Energy Agency.

Lanahan, M. & Tabares-Velasco, P. C., 2017. Seasonal thermal-energy storage: A critical review on BTES systems, modeling, and system design for higher system efficiency. *Energies.*

Sibbitt, B. et al., 2012. The performance of a high solar fraction seasonal storage district heating system - Five years of operation. *Energy Procedia,* Volume 30, pp. 856 - 865.